Journal of Basic and Environmental Sciences

ISSN
Online: 2356-6388
Print: 2536-9202

Research Article Open Access

Structure, Optical properties, and Thermal stability of Co_3O_4-Silicone Rubber as a solar selective absorber for solar thermal energy conversion

[1]T. Y. Elrasasi, [2] B. Abdalla, [1]M. Elmansy

[1] Physics Department, Faculty of Science, Benha University, Benha, Egypt

[2] Department of Basic Science, High Institute of Engineering and Technology in El-Arish, Egypt

*Corresponding author e-mail: tarek.elrasasi@fsc.bu.edu.eg

Mobile: +201010552665, ORCID: 0000-0002-2133-7724, SCOPUS ID: 35755304300

Abstract

In the present work, Cobalt tetra oxide (Co_3O_4) nanoparticles have been added to Silicon rubber (SiR) at different concentrations to be used as a solar selective material for thermal solar heaters. The prepared samples have been characterized by using XRD, FT-IR, SEM, TGA, and DSC. The absorbance and the emittance have been calculated from the reflection spectra of the UV-Vis-NIR in the range from 300 to 2500 nm. The investigated samples exhibited integral solar absorbance values of about 91% and emittance values of about 8.7%.

Keywords: Thermal solar energy, Selective absorber, Optical properties

---

1. Introduction

Climate change is one of the most critical problems these days that capture the thought and efforts of scientists to find a quick and effective solution. The main cause of this problem is the use of fossil fuels. On the other hand, the need for more energy continues to rise. Therefore, scientists are trying to find alternative clean, and sustainable sources of energy. Solar energy is one of the most promising renewable energy. It can be used to produce electricity directly via the photo volatile cells or thermal power plants, thermal solar heaters, and water desalination. Nowadays, many countries exert a lot of effort to switch the electric or gas heaters into thermal solar ones. Concentrating solar power (CSP) systems are the most important candidate for this purpose. Solar energy can be concentrated onto a highly absorbing material in the visible and near-infrared regions with low emissivity in the infrared portion of the solar spectrum [1]. The photo-thermal conversion efficiency of the CSP system depends on the progress of materials in the collector which can be improved by applying spectrally selective absorbing coatings with high solar absorptance and low thermal emittance over the entire solar spectrum range (0.3–2.5 μm) and infrared region (2.5–25 μm) respectively [1-3]. An ideal spectrally selective absorbing coating is characterized by high absorptance ($\alpha = 1$) and low emittance ($\varepsilon = 0$) at high operating temperatures in the visible and infrared wavelengths of the solar spectrum respectively [4]. However, achieving these characteristics is not possible using a single material. Therefore, different approaches such as absorber-reflector tandem and cermet coatings were used by various research groups [5–7]. Realizing optimal characteristics of selective absorbing coatings requires the synthesis of composite layers [8], optimizing their thickness and surface roughness [9–12].

In CSP, several components like concentrator, receiver, structure, heat transfer fluid, thermal insulation material, and other optical and mechanical components are involved to get maximum efficiency of the system. Out of all these

components, the solar receiver tube (SRT) plays a vital role to convert all solar radiation into heat [13]. SRT absorbs all the solar radiation in the wavelength region of 0.3–2.5 μm and converts them into thermal energy. The photothermal conversion efficiency of SRT majorly depends upon the solar absorber coating type. Therefore, the coating in the solar receiver tube must be chosen carefully [14]. The coating should absorb most of the incoming solar radiation and has the minimum emitting heat radiation. These properties like absorptance (α) and emittance (ε) can be measured at different wavelength regions depending upon the transition wavelength of the CSP operating temperature [15,16].

Polysiloxanes or silicone rubbers (SiR), which are the most common inorganic elastomers, utilize the siloxane functional group (Si–O–Si) in their backbone (see Fig. 1) [18]. Commercial silicone rubbers usually contain some organic side groups attached to the silicon atoms, which can promote cross-linking. The inorganic/organic hybrid nature of silicone rubbers provides them with a unique combination of properties, placing them in a material regime between silicate minerals and organic polymers with attributes of both sides [20]. The higher binding energy of Si–O bonds (~433 kJ mol^{-1}) compared to that of C–C bonds (~355 kJ mol^{-1}) results in greater heat resistance and thermal stability for this class of polymers [21,22]. Furthermore, structural features, such as higher bond length (Si–O: 1.64 ºA compared to C–C: 1.53 ºA) and relatively free rotation around Si–O–Si bond, result in very high chain flexibility and T_g values well below zero (~ − 125°C). The organic side groups also lead to the very low surface energy of the chains, imparting high hydrophobicity [22–24]. In addition to outstanding elasticity and a wide working temperature, SiR exhibits weatherability and better stability when exposed to ultraviolet radiation and corona discharge compared to organic polymers. SiR has very little water absorption even after long periods of submersion and can resist high-temperature oils as well. Furthermore, with very high resistance of 1–100 T Ω.m, SiR has significant electrical insulating performance over a wide frequency spectrum [21]. SiR's inert nature provides them with good biocompatibility as well [25]. Due to these excellent properties, SiR has found a special place in many industries such as aerospace and automotive, electronics, power transmission and distribution, household and leisure, food sector, building industry, health and medical, and pharmaceutical [25, 26].

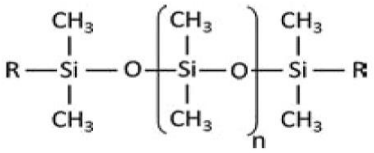

Fig 1. Chemical structure of a silicone rubber

In the present work, the objective of this study is the synthesis of polymeric solar selective absorber materials to be used in low-temperature solar collectors (≤100 °C) which consist of nano-structured Co_3O_4 embedded into SiR at different concentrations.

2. Experimental

2.1 Materials

Cobalt hydroxide (Co $(NO_3)_2$_$6H_2O$) was provided by QualiKems Chemical Company, India. Sodium hydroxide (NaOH) and Toluene were purchased from Adwic pharmaceutical and chemicals company Egypt.

2.2 Co_3O_4 preparation

Cobalt hydroxide b-Co $(OH)_2$ precursor was chemically precipitated by mixing cobalt nitrate (Co $(NO_3)2$_$6H_2O$) and sodium hydroxide (NaOH) aqueous solutions with continuous stirring [27,28]. The brown precipitate was separated by centrifugation after being washed several times with double distilled water to remove sodium nitrate ions and then dried in an oven at 383 K for 24 h. The color of the precipitates was turned black and Co_3O_4 crystallites are directly formed. To obtain Co_3O_4 nanoparticles of different sizes, the dried powder was calcined in an air atmosphere at different temperatures from 473 to 973 K for 3 hrs.

2.3 preparation of Co_3O_4-SiR as a solar selective absorber

An efficient new method for mixing nanoparticles and rubber [29] was used to get better dispersion of nanoparticles in coatings. In the new method (A) (see Fig. 2), nanoparticles were dispersed in the solvent, and then the dispersion was added to the silicone rubber. 20 gm of SiR dissolved in 400 ml Toluene (Tol) at 50 °C for one hour. The mixture has been filtered with filter paper. SiR/Tol. The solution has been stirred for another 6 hours after filtering. Co_3O_4 powder has been added wisely to 10 ml of the SiR/Tol. solution at different

concentrations (0, 0.05, 0.25 and 1 wt.%). The mixing process was done by using the magnetic stirrer for another two hours before using the ultrasonic device to break up any agglomerates. The samples have poured gently into Petri dishes and placed in the oven at 70 °C for two hours then left to dry for 72 hours at room temperature. The prepared samples were compressed in the form of tablets by hot press molding for curing at 170 °C under the pressure of 150 KPa for 10 min. The dimension of the tablet is 16 mm in diameter and 1.5 mm in thickness.

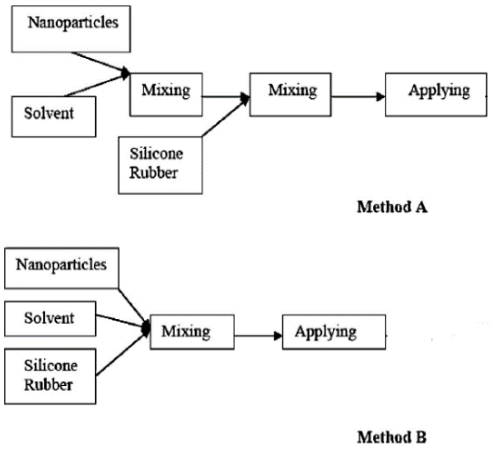

Fig. 2. The new mixing method (A) and usual mixing method (B) of coating production.

2.4 Characterization

The reflectance spectra of the coatings in the UV–Vis–NIR regions were measured using PerkinElmer Lambda 950 spectrophotometer. A high-resolution X-ray diffractometer (XRD) (Model APD 2000 PRO) was used to study the microstructure of Co3O4 absorber coating. The surface morphology of the film was investigated using Scanning Electron Microscope (SEM) (Model: FEI Nova Nano SEM 450). Fourier Transform Infrared Spectroscopy (FT-IR) (Model: TENSOR 27) was used to measure the infrared reflectance in the range of 5000–25000 nm. Thermal analysis (TGA) Thermogravimetric analysis, (DSC) Differential scanning calorimetry, and (DTA) Differential Thermal Analysis were studied by a thermal analyzer (Model: PerkinElmer TMA 4000).

3. Results and discussion

The crystal structure and the particle size of prepared Co_3O_4 have been examined by using the XRD technique, see Fig. 3. From the Figure, one can see the characteristic peaks of Co_3O_4. In Fig. 3, we notice the presence of peaks (111), (220), (311), (400), (422), (511), and (440) relating to Co_3O_4 material, located at 2θ equal to 18.90°, 31.30°, 36.81°, 44.90°, 55.70°, 59.50° and 64.92° respectively. The results found are in perfect agreement with the work of Patel et al. [30-32]. The crystallite size (D) of Co_3O_4 powder has been found to be 42 nm, was calculated by using Scherer Eq. (1)

$$D = \frac{0.9\,\lambda}{\beta\,cos\theta} \qquad (1)$$

Energy-dispersive X-ray spectrometry (EDX) analysis was employed to determine the composition of the Co_3O_4 NPs prepared. As shown in Fig. 4, the EDX spectrum of the product contains only oxygen and cobalt elements. No other elements can be detected in the spectrum, indicating the high purity of the Co_3O_4 nanoparticles. The experimental atomic percentages of Co and O are found to be 43.22% and 56.78%, respectively, which is near to the theoretical ratio (3:4) of Co_3O_4 [33].

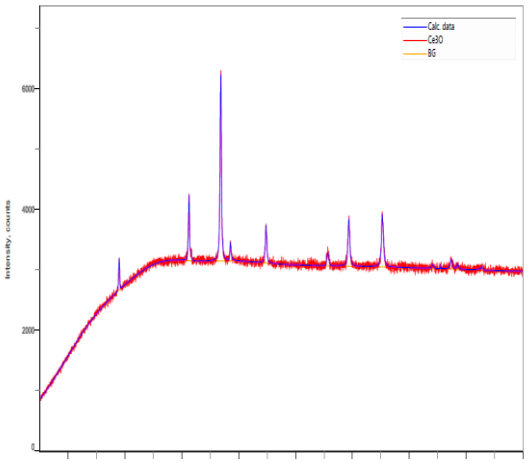

Fig. 3. XRD of Co_3O_4 prepared powder

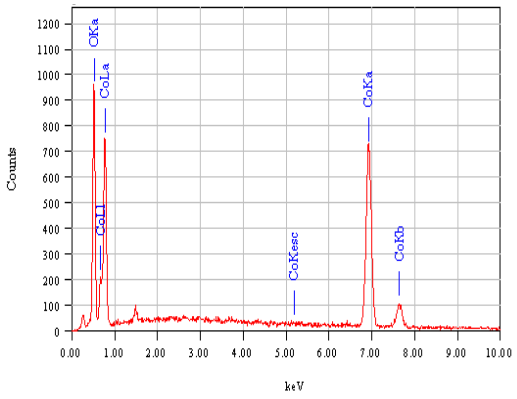

Fig. 4. EDX spectra of Co3O4 nanoparticles

Fig. 5 shows the X-ray diffraction pattern of Co_3O_4/SiR at different concentrations. A broad peak at 2θ = 20.6 ° which can be referred to as the silicone rubber peak position, results failed to find any significant differences between virgin SiR and the different concentrations of Co_3O_4. This may be due to the nanosize and the small percentage of prepared Co_3O_4 powder in the silicone rubber matrix. These results indicate that the microstructure of the samples was amorphous and that grafting did not change the bulk properties of the base aterial [34].

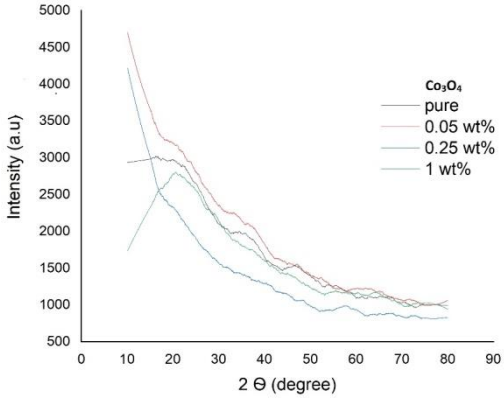

Fig. 5. XRD of Co_3O_4 -SiR solar selective absorber at different concentrations.

The FT-IR spectrum obtained from Co_3O_4-SiR solar selective absorber at different concentrations is illustrated in Fig. 5. The peaks observed at 3610 cm-1 characteristic peaks assigned to the cobalt-oxygen (Co–O) vibrational modes in Co_3O_4 we observed that the intensity of the peak in a steady value by the concentration of Co_3O_4 increase, the scan observed transmittance peaks at 3452 cm^{-1}, 2964 cm^{-1}, 1637 cm^{-1}, 1267 cm^{-1}, 1267 cm^{-1},1259 cm^{-1} and lastly at 802 cm^{-1}. The 3452 cm^{-1} corresponds to the stretching and bending vibrations for the hydroxyl (O–H) groups of water molecules present in the samples [34]. In the region 3450 cm^{-1} the intensity of absorption associated with O–H groups and free water increases (in turn reducing the transmittance) which can be directly related to the moisture content of the Co_3O_4. The bands located at 1637 cm^{-1} –1259 cm^{-1} correspond to a strong three bond alkyne group (C–C) and carbonyls (C = O). In the fingerprint region peaks 1018 cm^{-1} – 802 cm^{-1} indicate a strong presence of esters, ethers and carboxylic acids (C–C; C-O) bonds in the sample [35].

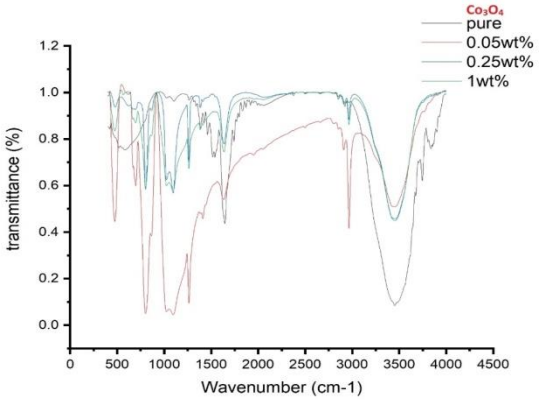

Fig 6. FT-IR spectrum of Co_3O_4 /SR solar selective absorber at different concentrations.

Fig. 7 illustrates TGA curves of Co_3O_4 /SiR composite at different concentrations. The initial weight change from the core/shell composites up to 230 ºC was probably due to the removal of surface hydroxyls and/or surface adsorbed water [37], the mass increased slightly due to the carboxylate groups being decomposed to CO_2 followed by re-adsorption by the coordination polymer, that indicating that the molecular structure has not changed and aging has not happened, so the samples showed good thermal stability up to 230 ºC [38]. The weight loss at higher temperatures (230–370 ºC) could be attributed mainly to the evaporation and subsequent decomposition of the amorphous carbon bonds and the SiR decomposition. The total amount of mass lost is about 5% of the starting mass. It has been observed that the sample (1wt%) showed the best thermal stability while the pure SiR sample (0 wt%) is the fastest in decomposition, which mean the thermal stability increase with the increase of Co_3O_4 concentration. Fig. 8 shows the results obtained from the DSC measurement of the prepared samples. There is no endothermic or exothermic peak appeared, also, there is no phase transformation occurring in the low temperature < 100 °C where glass transition occurs at about -127ºC [39]. These results are in agreement with TGA results, where the samples showed thermal stability at temperatures <100 °C.

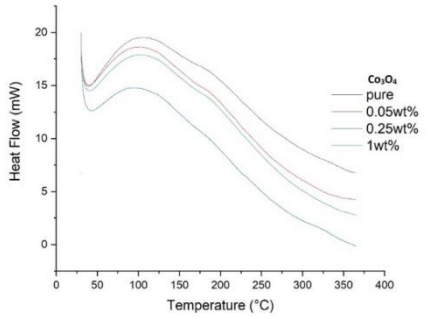

Fig. 7. TGA of Co_3O_4 /SR solar selective absorber at different concentrations.

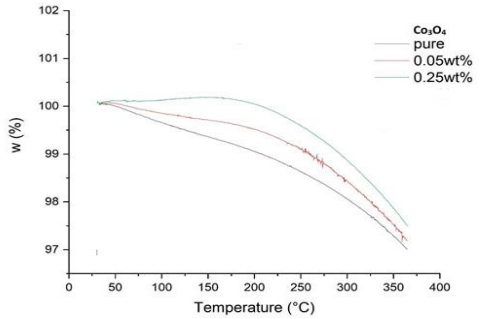

Fig. 8. DSC of Co_3O_4-SiR solar selective absorber at different concentrations.

Optical properties of the absorber coatings

The optical properties of the samples have been determined in the UV–Vis-NIR interval, for total reflectance (R(λ)) and transmittance (T(λ)) measurements. Absorptivity was obtained from the Eq. (2)

$$A(\lambda) = 1 - R(\lambda) - T(\lambda) \qquad (2)$$

where A(λ) is the absorptance, R(λ) is the total reflectance and T(λ) is the total transmittance.

The performance of the samples as selective solar coatings was characterized in terms of their spectral reflectance. The absorptance of a non-transparent material for a given temperature and wavelength is given by Eq. (3):

$$\alpha(\lambda, T) = 1 - (\lambda, T) \qquad (3)$$

And considering Kirchhoff's law of thermal radiation, the emittance for a given temperature and wavelength can be calculated according to Eq. (4):

$$\varepsilon(\lambda, T) = \alpha(\lambda, T) \qquad (4)$$

which is obtained from measurements of the spectral reflectance at the operating temperature. To calculate the total solar absorptance of the selective surface and thermal emittance Eqs. (5,6) expressions have been used

$$\alpha_{sol} = \frac{\int_{0.3\,\mu m}^{2.5\,\mu m} I_b(\lambda)(1-\rho(\lambda,T)d\lambda}{\int_{0.3\,\mu m}^{2.5\,\mu m} I_{sol}(\lambda)d\lambda} \qquad (5)$$

$$\varepsilon = \frac{\int_{0.3\,\mu m}^{2.5\,\mu m} I_{sol}(\lambda)(1-\rho(\lambda,T)d\lambda}{\int_{0.3\,\mu m}^{2.5\,\mu m} I_b(\lambda)d\lambda} \qquad (6)$$

where ρ(λ, T) is the spectral reflectance and $I_{sol}(\lambda)\, d\lambda$ is the normal spectral irradiance (AM 1.5 spectral irradiance for air mass 1.5), which is a standard of solar spectral radiation on the earth's surface and I_b is the spectral black body emissive power at room temperature [40,41]. The above expression describes the ability of the material to collect the solar energy it receives at the level of the earth's surface. Some expressions can be used to indicate the effectiveness of the selective surface. The first one is the selectivity (ξ) which is the relationship between solar absorptivity (α) and thermal emittance (ε) at temperature T (Eq. (7)).

$$\xi = \frac{\alpha}{\varepsilon} \qquad (7)$$

The reflectance measurements were carried out in diffuse reflectance conditions within the 300 – 2500 nm wavelength range and used to calculate the absorbance for these structures by using eq. 4. The measured absorbance results are in Fig. 9(a). To understand the room

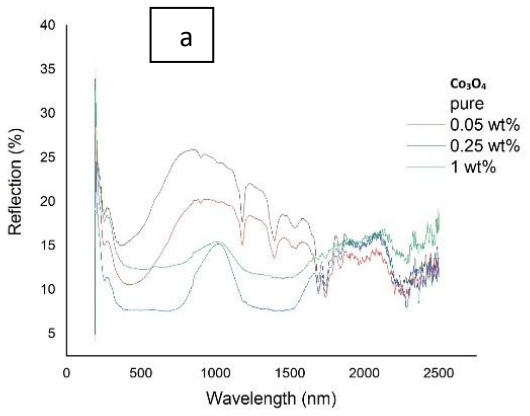

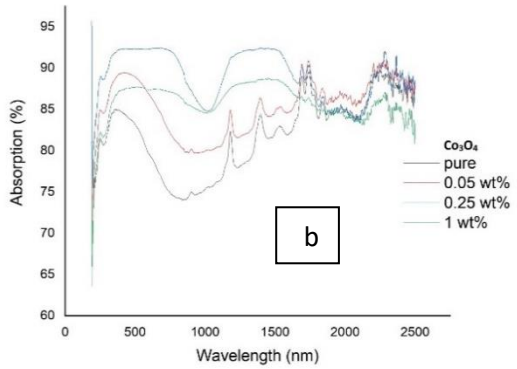

Fig. 9 UV-vis-NIR (a) Reflection and (b)Absorption spectra of Co_3O_4-SiR solar selective absorber at different concentrations.

temperature thermal emittance, we carried out reflectance measurements infrared region, which are plotted in Fig. 9(b) by using eq 5. Table 1 summarizes the values of selectivity parameters α, ε, and ξ [42].

Table 1. The absorption coefficient, emission coefficient, and selectivity of Co_3O_4-SiR solar selective absorber at different concentrations.

sample	α	ε	ξ
Pure	86.85 %	8.47 %	10.24
0.05 wt%	85.12 %	8.84 %	9.62
0.25 wt%	91.12 %	8.78 %	10.37
1 wt%	86.99 %	8.77 %	9.90

4. Conclusions

Co_3O_4 nanoparticles have been prepared and examined by XRD and EDX before impeding successfully inside a Silicone rubber as a polymeric nanocomposite matrix using a standard solvent-based technique to be used as a solar absorptance paint. Co_3O_4-SiR nanocomposite selective absorber has been investigated by measuring spectral reflectance. The solar absorptance of Co_3O_4-SR nanocomposite selective absorber up to 91% and thermal emittance about 8.7% for the optimum concentration of (0.25wt %). Thermal properties studies showed good thermal stability at low temperatures > 100°C.

3. References

[1] Zhao S, W¨ackelgård E. Optimization of solar absorbing three-layer coatings. Sol Energy Mater Sol Cells (2006)90:243–61. https://doi.org/10.1016/j.solmat.2005.03.009.

[2] Sani E, Mercatelli L, Meucci M, Balbo A, Silvestroni L, Sciti D. Compositional dependence of optical properties of zirconium, hafnium, and tantalum carbides for solar absorber applications. Sol Energy (2016)131:199–207. https://doi.org/10.1016/j.solener.2016.02.045

[3] Gao XH, Guo ZM, Geng QF, Ma PJ, Wang AQ, Liu G. Enhanced optical properties of TiN-based spectrally selective solar absorbers deposited at a high substrate temperature. Sol Energy Mater Sol Cells (2017)163:91–7. https://doi.org/10.1016/j.solmat.2017.01.023.

[4] Usmani B, Dixit A. Spectrally selective response of ZrOx/ZrC-ZrN/Zr absorber-reflector tandem structures on stainless steel and copper substrates for high temperature solar thermal applications. Sol Energy (2016)134:353–65. https://doi.org/10.1016/j.solener.2016.05.014.

[5] Dan A, Jyothi J, Chattopadhyay K, Barshilia HC, Basu B. Spectrally selective absorber coating of WAlN/WAlON/Al2O3 for solar thermal applications. Sol Energy Mater Sol Cells (2016)157:716–26. https://doi.org/10.1016/j.solmat.2016.07.018.

[6] Cao F, Kraemer D, Sun T, Lan Y, Chen G, Ren Z. Enhanced thermal stability of W-Ni-Al2O3 Cermet-based spectrally selective solar absorbers with tungsten infrared reflectors. Adv Energy Mater (2015)5:1–7. DOI: 10.1002/aenm.201401042.

[7] Tsai TK, Li YH, Fang JS. Spectral properties and thermal stability of CrN/CrON/ Al2O3 spectrally selective coating. Thin Solid Films (2016)615:91–6. https://doi.org/10.1016/j.tsf.2016.06.055.

[8] Craighead HG, Howard RE, Sweeney JE, Buhrman RA. Graded-index Pt-Al2O3 composite solar absorbers. Appl Phys Lett (1981)39:29–31. https://doi.org/10.1063/1.92552.

[9] Ning Y, Wang W, Sun Y, Wu Y, Liu Y, Man H, et al. Effects of substrates, film thickness and temperature on thermal emittance of Mo/substrate deposited by magnetron sputtering. Vacuum (2016)128:73–9. https://doi.org/10.1016/j.vacuum.2016.03.008.

[10] Sudipto P, Diso D, Franza S, Licciulli A, Rizzo L. Spectrally selective absorber coating from transition metal complex for efficient photothermal conversion. J Mater Sci (2013)48:8268–76. https://doi.org/10.1007/s10853-013-7639-4.

[11] Mahadik DB, Lakshmi RV, Barshilia HC. High performance single layer nano-porous antireflection coatings on glass by sol-gel process for solar energy applications. Sol Energy Mater Sol Cells (2015)140:61–8. https://doi.org/10.1016/j.solmat.2015.03.023.

[12] Wattoo AG, Song Z, Iqbal MZ, Rizwan M, Saeed A, Ahmad S, Ali A, Naz NA. Effect of zinc concentration on physical properties of copper oxide (Cu1/ xZnxO). J Mater Sci: Mater Electron (2015)26:9795–800. https:// DOI:10.1007/s10854-015-3651-6

[13] F. Cao, D. Kraemer, L. Tang, Y. Li, A.P. Litvinchuk, J. Bao, G. Chen, Z. Ren, A high-performance spectrally-selective solar absorber based on a yttria-stabilized zirconia cermet with high-temperature stability, Energy Environ. Sci. 8 (2015) 3040–3048. DOI: 10.1039/c5ee02066b

[14] C.G. Granqvist, Spectrally selective coatings for energy efficiency and solar applications, Phys. Scripta 32 (1985) 401–407.

[15] W.F. BOGAERTS, C.M. LAMPERT, Review Materials for photothermal solar energy conversion, J. Mater. Sci. 15 (1983) 2847–2875.

[16] M.H. Gray, R. Tirawat, K.A. Kessinger, P.F. Ndione, High temperature performance of high-efficiency, multi-layer solar selective coatings for tower applications, Energy Procedia 69 (2015) 398–404. https://doi.org/10.1016/j.egypro.2015.03.046

[17] U. Schwertmann, R.M. Cornell, The Iron Oxide: Structure, Properties, Reactions, Occurrence and Uses, second ed., Wiley–VCH, Denmark, (2003) ISBN: 978-3-527-60644-3

[18] Polymers and Plastics: An Introduction to their structures and properties. http://www.chem1.com/acad/webtext/states/polymers.html (accessed March 23, 2017).

[19] Sovar, R. D. Novel Analytical Techniques for the Assessment of Degradation of Silicone Elastomers in High Voltage Applications; Queensland University of Technology, 2004.

[20] Goudie, J.; Owen, M.; Orbeck, T. A Review of Possible Degradation Mechanisms of Silicone Elastomers in High Voltage Applications. Annual Report of the 1998 Conference on Electrical Insulation and Dielectric Phenomena, Atlanta, Georgia, USA. IEEE 0–7803- 5035–9. DOI: 10.1109/CEIDP.1998.733878

[21] Characteristic Properties of Silicone Rubber Compounds, Shin-Etsu Chemical Co. Ltd., Japan. HTTP://www.shinetsusilicone-global.com/catalog/pdf/rubber_e. pdf, 2012 (accessed April 06, 2017).

[22] Mark, J.E. Some Interesting Things about Polysiloxanes. Acc. Chem. Res. 2004, 37(12), 946–953. https://doi.org/10.1021/ar030279z

[23] Mark, J. E.; Lin, G.; Schaefer, D. W. The Polysiloxanes; Oxford University Press, New York, 2015.

[24] Dow. Silicones in the Electronics Industries. http://www.dowcorning.com/content/publishedlit/chapter11.pdf (accessed April 06, 2017).

[25] Jerschow, P. Silicone Elastomers; Rapra Technology Limited, Report 137, 2001; 12(5).

[26] Colas, A. Silicones: Preparation, Properties and Performance; Dow Corning, Life Sciences, 2005, pp 1–14.

[27]O.A. Fouad, S.A. Makhlouf, G.A.M. Ali, A.Y. El-Sayed, Mater. Chem. Phys. 128 (2011) 70–76.

[28]Salah A. Makhlouf a,c,⇑, Zinab H. Bakr a, Kamal I. Aly b, M.S. Moustafa Structural, electrical and optical properties of Co3O4 nanoparticles

Superlattices and Microstructures 64 (2013) 107–117

[29] H. Acharya, S.K. Srivastava, EPDM/Silicone Blend Layered Silicate Nanocomposite by Solution Intercalation Method: Morphology and Properties, polymer composite 35 (2014) 1834-1841 https://doi.org/10.1002/pc.22848

[30] Avila, A.G., Barrera, E.C., Huerta, L.A., Muhl, S. (2004). Cobalt oxide films for solar selective surfaces, obtained by spray pyrolisis. Solar Energy Materials & Solar Cells, 82(1-2): 269-278. http://doi.org/10.1016/j.solmat.2004.01.024.

[31] Patil, V., Joshi, P., Chougule, M., Sen S. (2012). Synthesis and characterization of Co3O4 thin film. Soft Nanoscience Letters, 2(1): 1-7. https://doi.org/10.4236/snl.2012.21001.

[32] Patel, M., Kim, J. (2018). Thickness-dependent photoelectrochemical properties of a semitransparent Co3O4 photocathode. Beilstein Journal of Nanotechnology, 9: 2432-2442. https://doi.org/10.3762/bjnano.9.228.

[33] S. Farhadi*, A. Sepahdar, K. Jahanara , Spinel-Type Cobalt Oxide (Co3O4) Nanoparticles from the mer-Co(NH3)3(NO2)3 Complex: Preparation, Characterization, and Study of Optical and Magnetic Properties , JNS 3 (2013) 199- 207

[34] Bai C, Zhang X, Dai J, and Wang J 2008 Diketopyrrolopyrrole-based conjugated polymers as additives to optimize morphology for polymer solar cells Chinese Journal of Polymer Science volume 34, pages491–504 (2016)

[35] I. Luisetto, F. Pepe, E. Bemporad, J. Nanopart. Res. 10 (2008) 59–67.

[36] C.-W. Tang, C.-B. Wang, S.-H. Chien, Thermochim. Acta. 473 (2008) 68–73.

[37] Bin Zhang, Yunchen Du, Peng Zhang, Hongtao Zhao, Leilei Kang, Xijiang Han, Ping Xu Microwave Absorption Enhancement of Fe3O4/Polyaniline Core/Shell Hybrid Microspheres with Controlled Shell Thickness Chinese Journal of Polymer Science Vol. 34, No. 4, (2016), 491–504. doi: 10.1007/s10118-016-1761-0

[38] Zhigao Wang, Xinghai Zhang, Fangqiang Wang & Xinsheng Lan (2016): Chemical characterization and research on the silicone rubber material used for outdoor current transformer insulation, Phosphorus, Sulfur, and Silicon and the Related Elements, DOI:10.1080/10426507.2016.1231189

[39] A. Sasikala, A. Kala Characterization of some selected vulcanized and raw silicon rubber materials AIP Conference Proceedings 1849, 020048 (2017); doi: 10.1063/1.4984195.

[40] W.F. BOGAERTS, C.M. LAMPERT, Review Materials for photothermal solar energy conversion, J. Mater. Sci. 15 (1983) 2847–2875.

[41] M.H. Gray, R. Tirawat, K.A. Kessinger, P.F. Ndione, High temperature performance of high-efficiency, multi-layer solar selective coatings for tower applications, Energy Procedia 69 (2015) 398–404.

[42] Ajoy K. Saha1, Rajesh Kumar1,2, Belal Usmani1,2, Laltu Chandra1,3, Ambesh Dixit1,2, Development of nickel modified Fe3O4 solar selective coatings for solar absorber applications Advanced Materials Proceedings 1(2)140-145 (2016) DOI: 10.5185/amp.2016/205